



Figures and figure supplements

An intrinsic cell cycle timer terminates limb bud outgrowth

Joseph Pickering et al

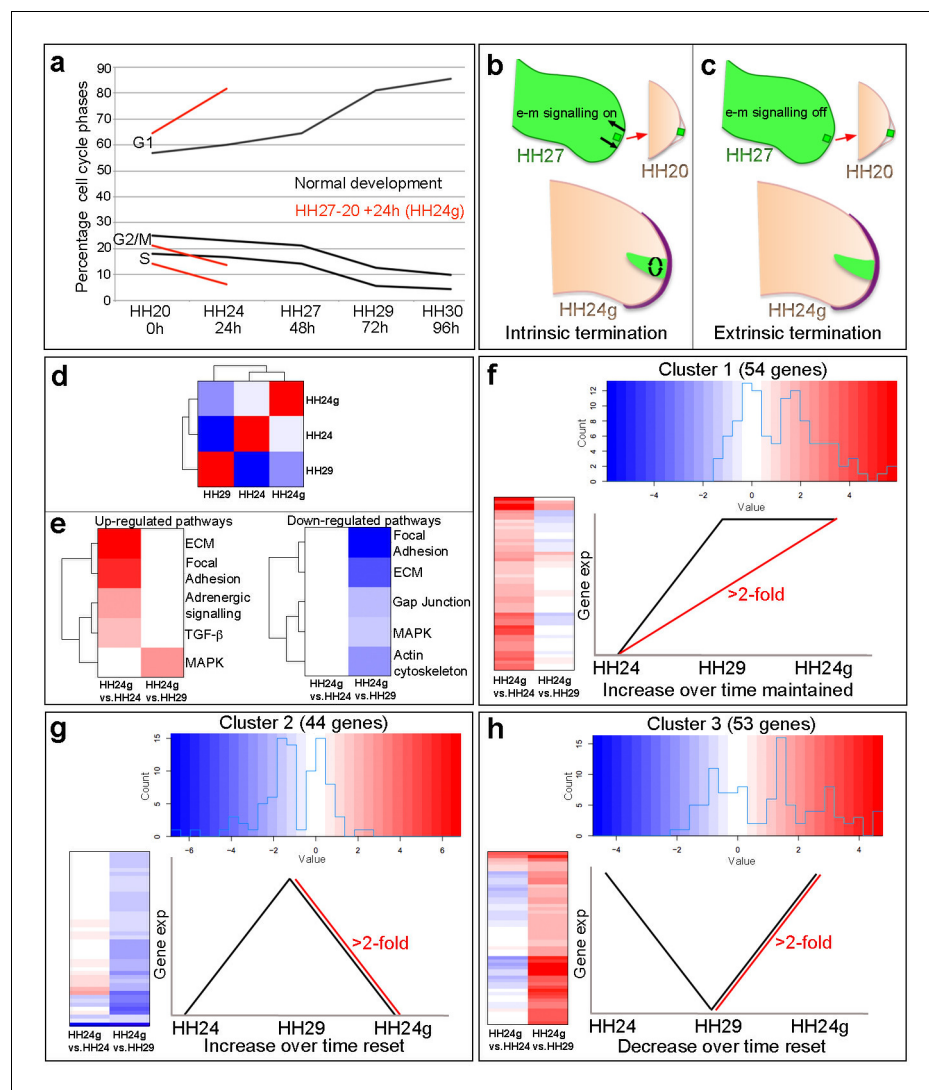


Figure 1. Cell cycle and RNA-seq analyses of chick wing distal tips. (a) Decline in cell cycle rate determined by proportions of cells in G1-, S- and G2/M-phases between HH20 and HH30 in the distal chick wing bud (black lines [Saiz-Lopez et al., 2017](#)). Red lines show maintenance of cell cycle program in grafts of HH27 distal tips made to HH20 wing buds left for 24 hr until HH24 (HH24g - tissue would have progressed from HH27 to HH29 in donor) – note trajectories follow same pattern as black lines between HH27 and HH29. (b–c) Procedure for making HH27-20 grafts ([Saiz-Lopez et al., 2017](#)) and predictions for loss of proliferative growth in HH24g mesenchyme. (b) Intrinsic termination: e-m signalling (arrows in HH27 wing bud) maintained between mesenchyme and apical ridge but proliferation declines intrinsically in mesenchyme independently of e-m signalling (curved arrows in HH24g mesenchyme). (c) Extrinsic termination: e-m signalling irreversibly lost between graft and apical ridge in HH27 bud (arrows absent) and proliferation lost in graft. (d) Heat-map showing the correlation (Pearson) of the normalised RNA-seq data collapsed to the mean expression per group and the degree of correlation indicated by the colour (red: higher, blue: lower). (e) KEGG analyses across pairwise contrasts with degree in pathway change indicated by the colour (red: up-regulated, blue: down-regulated). (f–h) Clustering of RNA-seq data across pairwise contrasts with degree of gene expression change indicated by the colour (red: higher, blue: lower). (f) Cluster 1: genes that increase between HH24 and HH29 (black line) and are maintained in HH24g (red line - > 2 fold higher in HH24g than HH24). (g) Cluster 2: genes that increase between HH24 and HH29 (black line) and reset in HH24g (red line - > 2 fold lower in HH24g than HH29). (h) Cluster 3: genes that decrease between HH24 and HH29 (black line) and reset in HH24g (red line - > 2 fold higher in HH24g than HH29).

DOI: <https://doi.org/10.7554/eLife.37429.002>

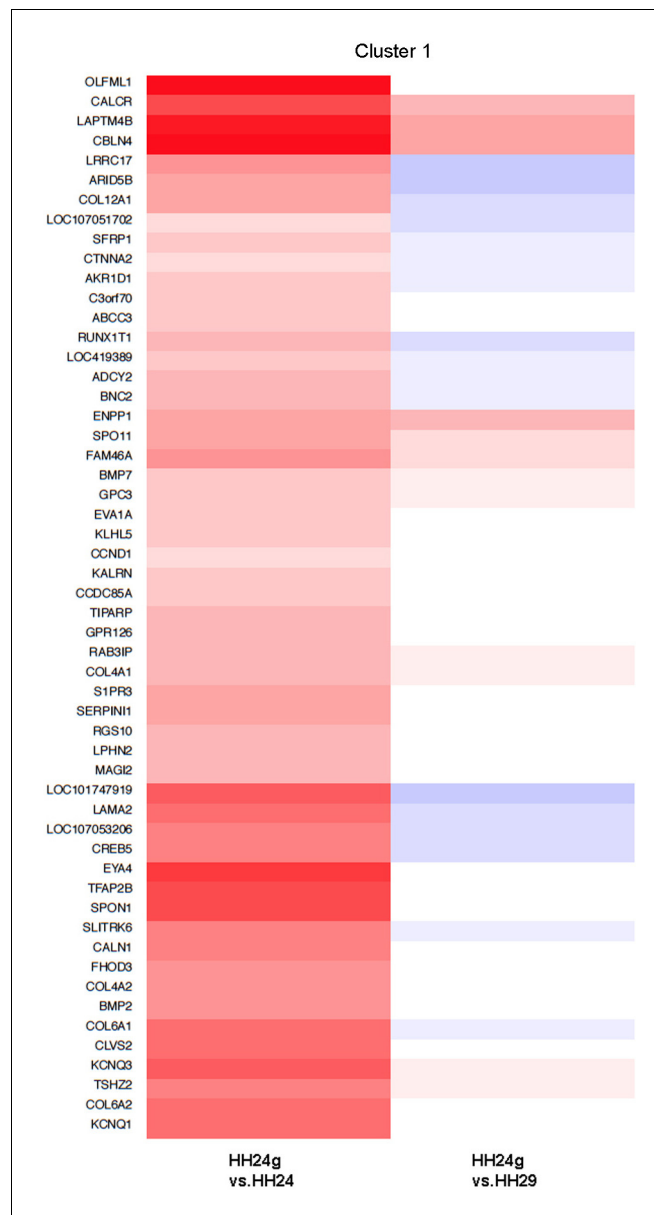


Figure 1—figure supplement 1. Cluster 1 Clustering of RNA-seq data across pairwise contrasts with degree of gene expression change indicated by the colour (red: higher, blue: lower). Cluster 1: genes that increase between HH24 and HH29 (black line) and are maintained in HH24g distal mesenchyme (red line - > 2 fold higher in HH24g than HH24).

DOI: <https://doi.org/10.7554/eLife.37429.003>

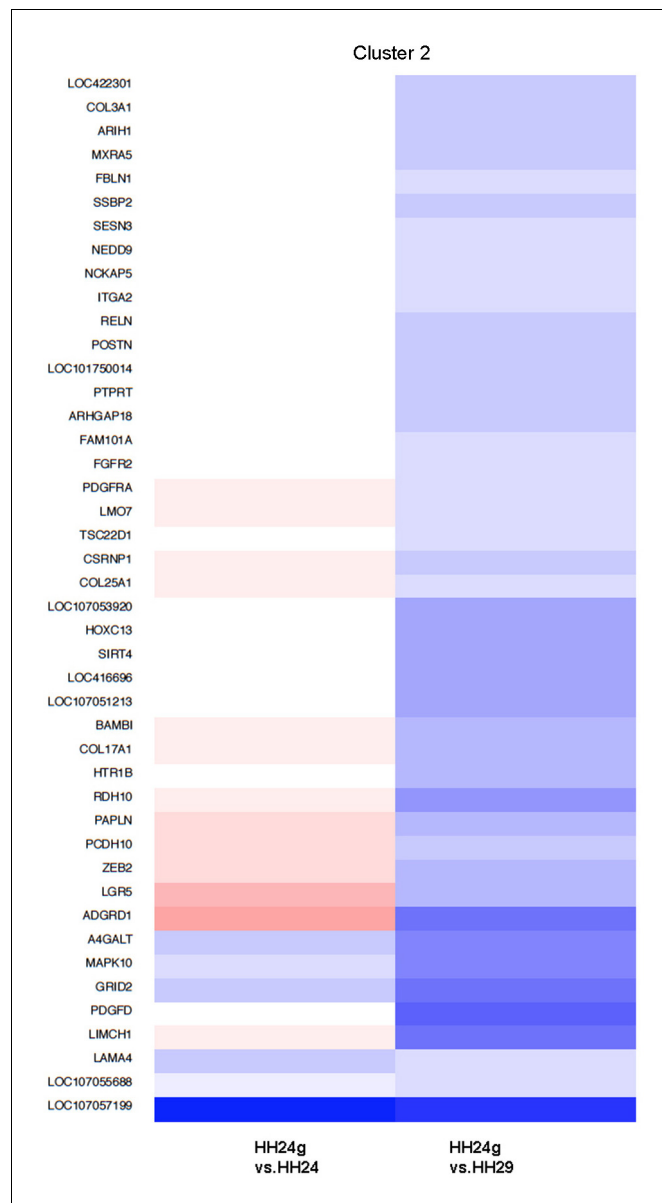


Figure 1—figure supplement 2. Cluster 2 Clustering of RNA-seq data across pairwise contrasts with degree of gene expression change indicated by the colour (red: higher, blue: lower). Cluster 2: genes that increase between HH24 and HH29 (black line) and reset in HH24g distal mesenchyme (red line - > 2 fold lower in HH24g than HH29). DOI: <https://doi.org/10.7554/eLife.37429.004>

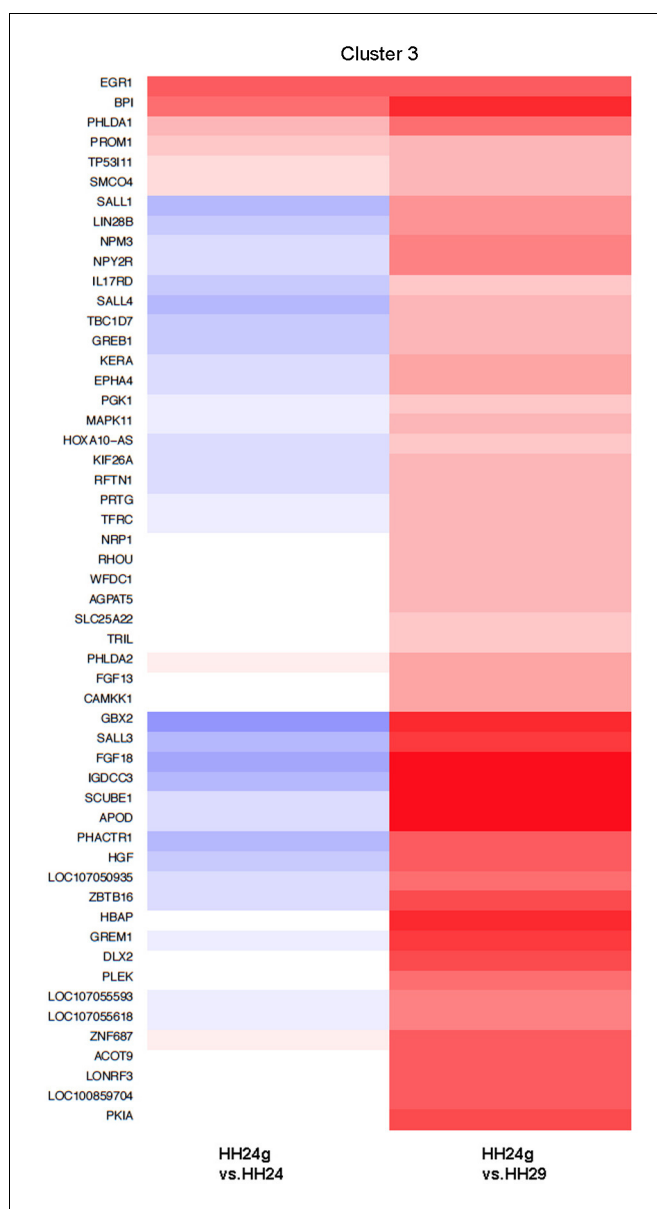


Figure 1—figure supplement 3. Cluster 3 Clustering of RNA-seq data across pairwise contrasts with degree of gene expression change indicated by the colour (red: higher, blue: lower). Cluster 3: genes that decrease between HH24 and HH29 (black line) and reset in HH24g distal mesenchyme (red line - > 2 fold higher in HH24g than HH29).

DOI: <https://doi.org/10.7554/eLife.37429.005>

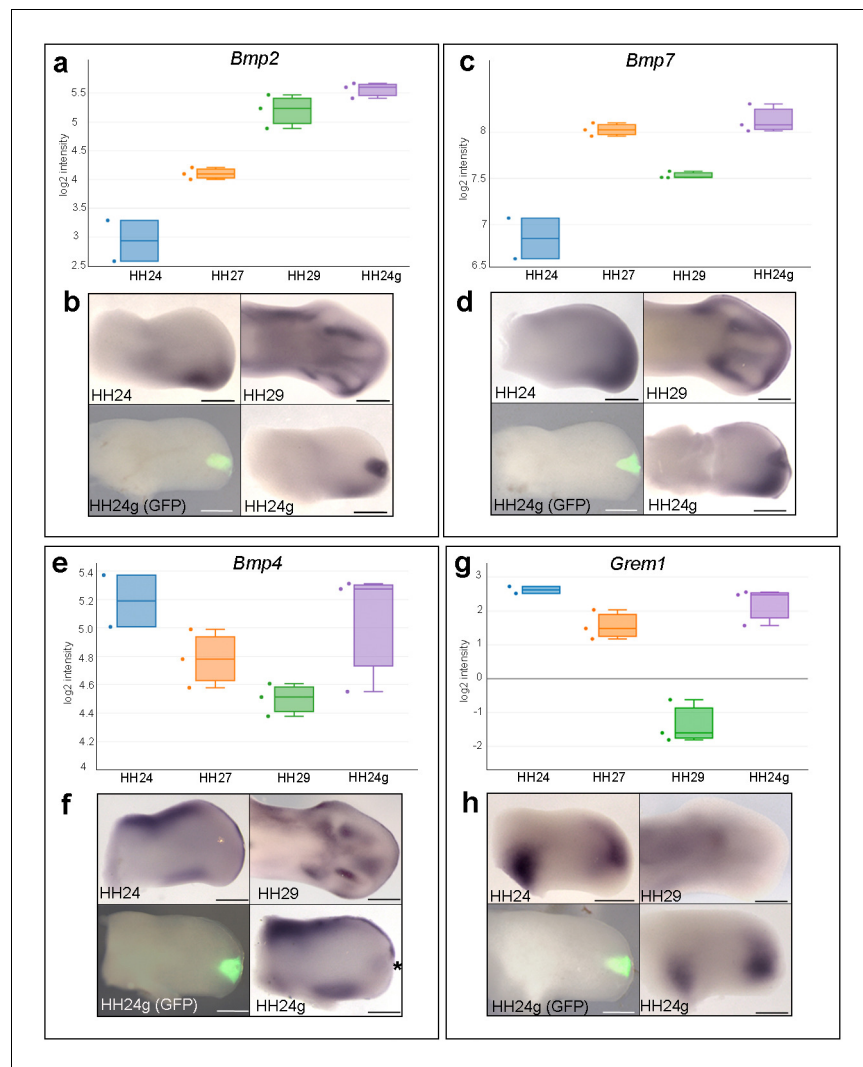


Figure 2. *Bmp2/4/7* and *Grem1* expression in HH24g mesenchyme. (a) Histogram showing expression levels of *Bmp2* as normalised log₂ values of RNA sequencing read-count intensities. (b) In situ hybridization showing *Bmp2* expression - note intense expression in HH24g mesenchyme in area of graft ($n = 3/3$, HH24 is the contralateral bud flipped horizontally). (c) Expression levels of *Bmp7* determined by RNA-seq. (d) In situ hybridization showing *Bmp7* expression - note intense region of expression in HH24g mesenchyme ($n = 3/3$). (e) Expression levels of *Bmp4* determined by RNA-seq. (f) In situ hybridizations showing *Bmp4* expression - note enhanced expression in HH24g mesenchyme in area of graft (asterisk - $n = 2/3$). (g) Expression levels of *Grem1* determined by RNA-seq. (h) In situ hybridizations showing resetting of *Grem1* expression ($n = 7/9$). Scale bars: HH24 buds - 500 μm ; HH29 buds - 200 μm .

DOI: <https://doi.org/10.7554/eLife.37429.006>

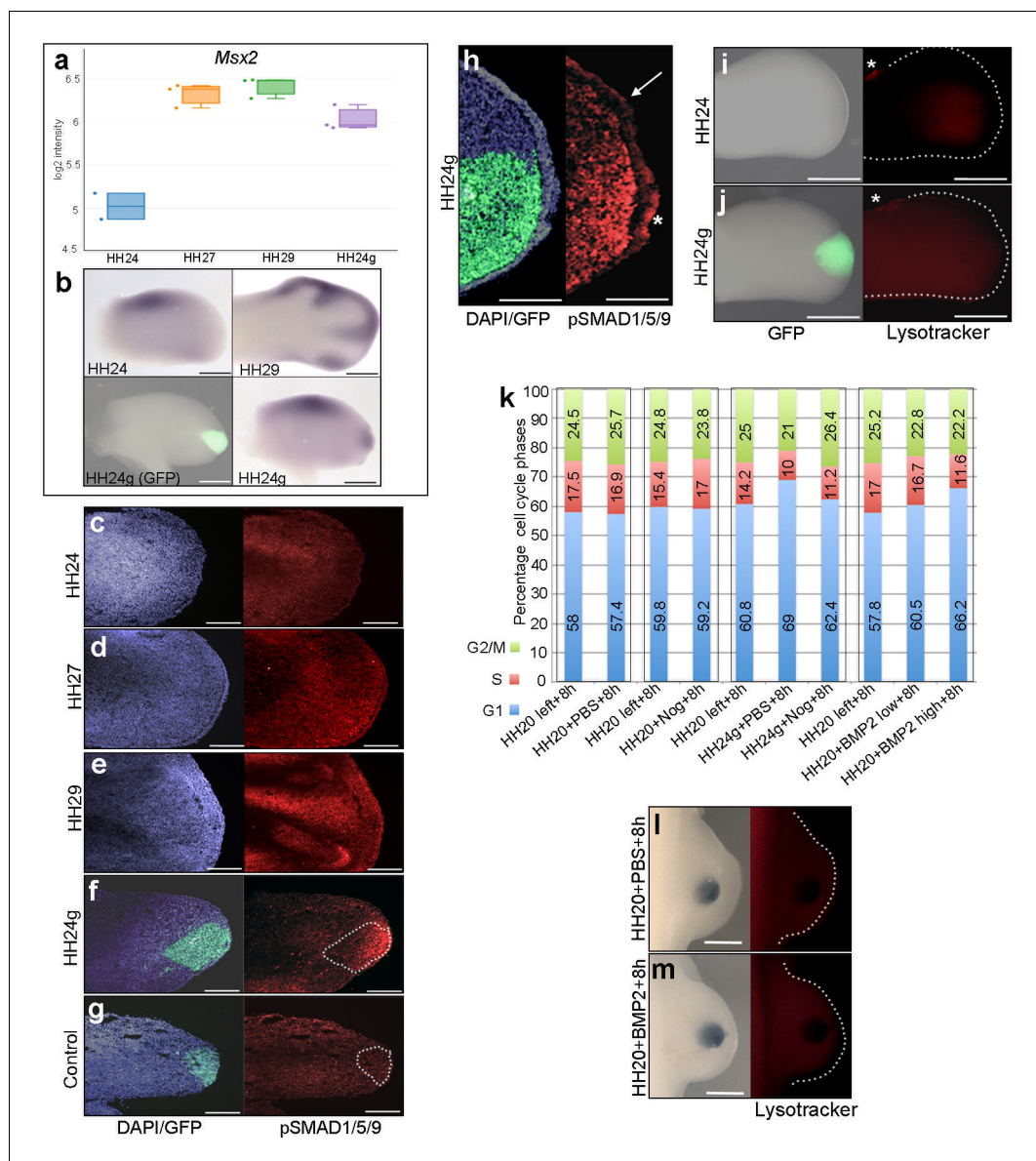


Figure 3. BMP signalling in HH24g mesenchyme (a) Expression levels of *Msx2* determined by RNA-seq. (b) In situ hybridization showing *Msx2* expression - note intense expression in HH24g mesenchyme in grafted area ($n = 3/4$). (c–h) Immunostaining of pSMAD1/5/9: signal increases in the distal part of chick wing buds over time (c–e) and is enhanced in HH24g mesenchyme (f) compared to contralateral HH24 buds ($n = 3/3$ c) but not in HH20-HH20 grafts ($n = 2/2$ g); signal is enhanced in apical ectodermal ridge above grafts in HH24g mesenchyme (asterisk-h) but not adjacent regions of ridge ($n = 2/2$ - arrow-h). (i–j) Lysotracker staining of apoptotic cells reveals no difference in HH24 (i) and HH24g (j) mesenchyme ($n = 5/5$) – asterisks indicate anterior necrotic zone. (k) Flow cytometry of wing bud distal mesenchyme: PBS- and Noggin-soaked beads do not significantly affect proportion of cells in G1-phase after 8 hr compared to left wing controls (Pearson's χ^2 test – $p=0.1$ and $p=0.4$, respectively); Noggin-soaked beads implanted at HH20 (+Nog) produce a significant decrease in proportion of cells in G1-phase in HH24g grafts compared to PBS-treated controls (+PBS) after 8 hr (Pearson's χ^2 test – $p<0.0001$); BMP2-soaked beads implanted at HH20 significantly increase G1-phase cells after 8 hr compared to left wing controls (Pearson's χ^2 test – $p<0.0001$), note boxes indicate separate experiments. (l–m) Lysotracker staining of apoptotic cells reveals no difference in PBS (l) – $n = 2/2$ and BMP2 (m) – $n = 2/2$ treated mesenchyme after 8 hr. Scale bars: HH24 buds – 500 μm , HH29 buds – 200 μm in b; 150 μm in c–g; 75 μm in h; 300 μm in i–j and l–m.

DOI: <https://doi.org/10.7554/eLife.37429.007>

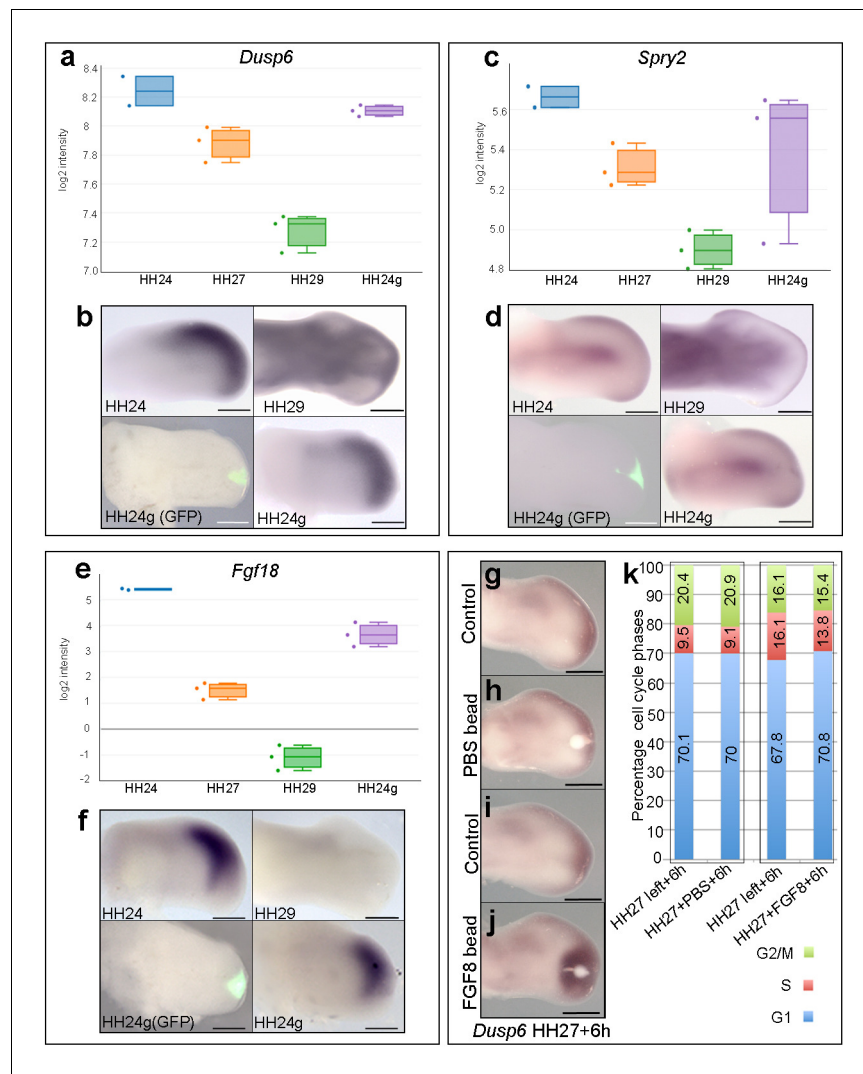


Figure 4. FGF signalling in HH24g mesenchyme. (a-e) Resetting of gene expression in HH24g mesenchyme. Expression levels of *Dusp6* (a), *Spry2* (c) and *Fgf18* (e) determined by RNA-seq. (b) In situ hybridization showing equivalent levels of *Dusp6* ($n = 3/3$), (b), *Spry2* ($n = 3/3$), (d), and *Fgf18* ($n = 3/3$), (f) in HH24 and contralateral HH24g mesenchyme. (g-j) FGF-soaked beads (j) $n = 3/3$), but not PBS-soaked beads (h) $n = 3/3$), up-regulate expression of *Dusp6* after 6 hr (control left wing buds flipped horizontally – (g) and (i)). (k) Flow cytometry of wing bud distal mesenchyme: PBS-soaked beads do not significantly affect proportion of cells in G1-phase after 6 hr compared to left wing controls (Pearson's χ^2 test – $p=0.5$); FGF-soaked beads implanted at HH27 significantly increase G1-phase cells compared to left wing control after 6 hr (Pearson's χ^2 test – $p<0.0001$), note boxes indicate separate experiments. Scale bars: HH24 buds, HH27 buds - 300 μm ; HH29 buds - 200 μm .

DOI: <https://doi.org/10.7554/eLife.37429.009>

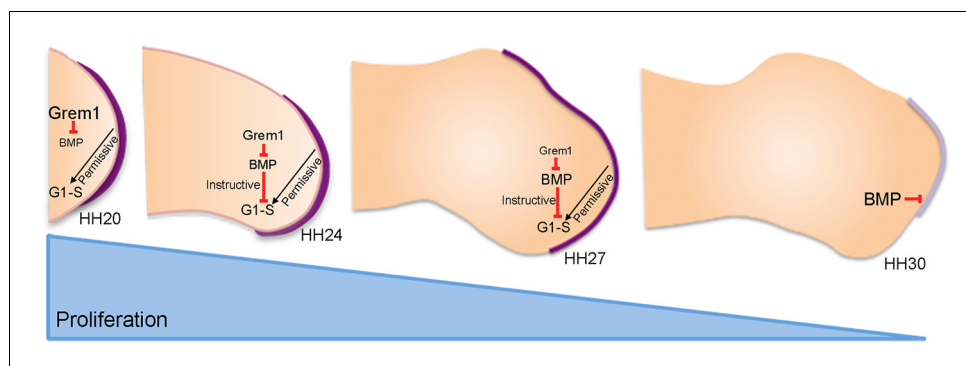


Figure 5. An intrinsic cell cycle timer terminates limb bud outgrowth. HH20-HH24: antagonism of BMP signalling by Grem1 permits rapid mesenchyme proliferation and maintenance of the apical ectodermal ridge (purple) that permissively supports outgrowth. HH24-HH27: intrinsic rise in BMP signalling counters BMP antagonism and instructively decelerates mesenchyme proliferation rate. HH27-HH30: mesenchyme proliferation diminishes as patterning completes at HH28 and then BMP signalling inhibits FGF signalling in apical ectodermal ridge that then regresses.

DOI: <https://doi.org/10.7554/eLife.37429.011>